ORIGINAL ARTICLE

In vivo brain macromolecule signals in healthy and glioblastoma mouse models: [1]H magnetic resonance spectroscopy, post–processing and metabolite quantification at 14.1 T

Mélanie Craveiro,* Virginie Clément-Schatlo,† Denis Marino,†
Rolf Gruetter*,‡,§ and Cristina Cudalbu¶

*Laboratory for Functional and Metabolic Imaging, Ecole Polytechnique Fédérale de Lausanne, Lausanne, Switzerland

†Department of Clinical Neurosciences, University of Geneva, Geneva, Switzerland

‡Department of Radiology, University of Lausanne, Lausanne, Switzerland

§Department of Radiology, University of Geneva, Geneva, Switzerland

¶Centre d'Imagerie Biomédicale, Ecole Polytechnique Fédérale de Lausanne, Lausanne, Switzerland

Abstract

In ^{1}H magnetic resonance spectroscopy, macromolecule signals underlay metabolite signals, and knowing their contribution is necessary for reliable metabolite quantification. When macromolecule signals are measured using an inversion-recovery pulse sequence, special care needs to be taken to correctly remove residual metabolite signals to obtain a pure macromolecule spectrum. Furthermore, since a single spectrum is commonly used for quantification in multiple experiments, the impact of potential macromolecule signal variability, because of regional differences or pathologies, on metabolite quantification has to be assessed. In this study, we introduced a novel method to post-process measured macromolecule signals that offers a flexible and robust way of removing residual metabolite signals.

This method was applied to investigate regional differences in the mouse brain macromolecule signals that may affect metabolite quantification when not taken into account. However, since no significant differences in metabolite quantification were detected, it was concluded that a single macromolecule spectrum can be generally used for the quantification of healthy mouse brain spectra. Alternatively, the study of a mouse model of human glioma showed several alterations of the macromolecule spectrum, including, but not limited to, increased mobile lipid signals, which had to be taken into account to avoid significant metabolite quantification errors.

Keywords: [1]H magnetic resonance spectroscopy, glioma, macromolecule.

J. Neurochem. (2014) **129**, 806–815.

Over the last decade, proton magnetic resonance spectroscopy (^{1}H MRS) research has benefitted from the development of ultrahigh field strength magnets, which allowed the quantification of an increased amount of up to 20 brain metabolites, which constitute the neurochemical profile (Pfeuffer *et al.* 1999; Mlynarik *et al.* 2008). In addition to brain metabolites, macromolecule (MM) resonances, which are mainly ascribed to cytosolic proteins and mobile lipids in certain pathological conditions (Kauppinen *et al.* 1992, 1993; Behar and Ogino 1993; Howe *et al.* 2003; Seeger *et al.* 2003; Opstad *et al.* 2010), are also detected using ^{1}H MRS and consist of broad resonances that overlap with the metabolite signals. However, the short relaxation times of MM protons allow their signals to be discriminated from

those of metabolites, which have longer relaxation times and narrower linewidths. At low magnetic field strengths, such as 1.5 T and 3 T, the broad MM signals have thus been successfully estimated using mathematical functions such as splines or wavelets (Soher *et al.* 2001; Schaller *et al.* 2013).

At increasing magnetic field strengths, however, more MM resonances can be distinguished (Otazo *et al.* 2006) and the increasing metabolite linewidth complicates a clear differentiation between the MM and *J*-coupled metabolite signals as it has been shown using the inversion-recovery (IR) technique and diffusion-weighted MRS at 14.1 T (Cudalbu *et al.* 2009b; Kunz *et al.* 2010). It has also been shown that an inadequate MM estimation at higher magnetic field strengths, using splines or truncation of the first points of the FID, for instance, may compromise a reliable metabolite quantification (Cudalbu *et al.* 2007, 2009b; Gottschalk *et al.* 2008; Mlynarik *et al.* 2008; Hong and Pohmann 2013). Consequently, new strategies have been developed to estimate MM signals at ultrahigh magnetic field strength, including measurement of MM signals (Pfeuffer *et al.* 1999; Mlynarik *et al.* 2008; Cudalbu *et al.* 2009b) or simulation of the MM components based on parameterization of prior knowledge obtained from measured MM signals (Seeger *et al.* 2003; Hong *et al.* 2011). Although measured MM signals have been widely used in brain metabolite quantification in previous studies (Pfeuffer *et al.* 1999; Mlynarik *et al.* 2008), attention has to be paid to the fact that regional differences or pathological conditions may affect the MM signals.

Previous studies have shown regional differences in metabolite levels in the brain of animals and humans (Tkac *et al.* 2003; Lei *et al.* 2010; Xin *et al.* 2010b), although only few studies have focused on regional differences at the MM level. A previous study in rats has shown no significant differences in the MM signals in several regions of the brain (Xin *et al.* 2010a). Studies conducted in humans have found slight differences in MM contribution in different brain locations, possibly because of differences in white/gray matter content (Mader *et al.* 2002). However, a study performed at 7 T recently showed that MM differences observed between gray and white matter did not significantly affect the ^{1}H MRS metabolite quantification (Schaller *et al.* 2012). Since a thorough investigation of MM variability has not yet been performed in the mouse brain, although the mouse brain is histologically more homogeneous with much smaller white matter content than the human brain, it is still unclear if potential regional differences, independently of gray/white matter content differences, in MM contribution may significantly affect ^{1}H MRS metabolite quantification in the mouse brain. This knowledge is especially important when a single brain MM spectrum is used for the investigation of several brain regions because of the significant amount of time that the measurement of the MM contribution can require.

While many pathological conditions are associated with metabolite level alterations, only a few of them, including multiple sclerosis, stroke, and brain tumors, have so far been investigated and linked to MM signal changes, which have been ascribed to increases of mobile lipids (Graham *et al.* 2001; Mader *et al.* 2001; Howe *et al.* 2003; Seeger *et al.* 2003; Opstad *et al.* 2010). The increase in mobile lipid signals observed in high-grade brain tumors has been linked with malignancy (Murphy *et al.* 2003; Fan *et al.* 2004) and has been associated with the extent of necrosis (Kuesel *et al.* 1994). An increase in mobile lipids has also been shown to correlate with cell death and apoptosis (Hakumaki *et al.* 1999). However, while several studies of high-grade gliomas in humans and animal models have reported increases in mobile lipids in the affected tissue (Howe *et al.* 2003; Opstad *et al.* 2010), acquisition of metabolite-nulled spectra was rarely performed and only at low magnetic field strength (Seeger *et al.* 2003). None of these studies, therefore, was able to report potential MM changes in the spectral region where visual separation of MM from the metabolite signals is not possible. An accurate measurement of the MM contribution at high magnetic field strength may, therefore, provide such information.

One drawback of measuring MM signals is the amount of time needed for establishing their contribution when investigating small regions of interest such as the mouse brain, especially when each subject is expected to express different MM alterations. Although this limiting factor is reduced when investigating bigger brain structures such as the human brain, a faster alternative to the MM measurement in each subject is offered by the possibility of simulating MM signals based on their parameterization (Seeger *et al.* 2003; Hong *et al.* 2011). However, even in that case, a preliminary precise measurement of the MM signals is still necessary for correct assessment of the prior knowledge necessary for their parameterization in given physiological or pathological conditions.

The measurement of MM signals has traditionally been performed using an IR sequence (Pfeuffer *et al.* 1999; Mlynarik *et al.* 2008; Cudalbu *et al.* 2009b) with an inversion time (TI) that allows an almost complete nulling of the metabolite signals, while the MM signals, which have shorter longitudinal relaxation times than metabolites, have almost completely recovered. However, because of the different longitudinal relaxation times of the metabolites (de Graaf *et al.* 2006; Cudalbu *et al.* 2009a), their complete nulling is typically difficult to achieve. Hence, an accurate *in vivo* determination of MM depends on the effective removal of the residual metabolite signals. Until now, this step has been performed using HLSVD (Hankel-Lanczos Singular Value Decomposition) (Pijnappel *et al.* 1992), which allows the selective removal of frequency components but does not offer any flexibility when these components overlap with MM signals of similar linewidth.

The primary aim of this study was, therefore, to establish an improved *in vivo* measurement of the MM component by implementing a method that can provide an accurate separation and removal of metabolite residuals from the MM components using prior knowledge of their frequency and linewidth, even in the case of similar linewidths. A secondary aim was to use this new method to measure MM signals in different regions of healthy mouse brains to detect potential regional differences that may affect metabolite quantification if not taken into account. Finally, a third aim was to study a mouse model of glioma derived from human glioma-initiating cells (GIC) to detect whether MM alterations may be induced by this pathology and thus should be taken into account for accurate metabolite quantification.

Material and methods

Female adult NOD-scid mice (Charles River Laboratories Inc., L'Arbresle, France), 6 weeks old, were housed in a 12 h light/dark cycle, with *ad libitum* access to food and water. Protocols were conform to Swiss legislation and the European Community Council directive (86/609/EEC) for the care and use of laboratory animals and conducted in compliance with ARRIVE (Animal Research: Reporting *In Vivo* Experiments) guidelines. All animal studies were approved by the local animal ethics committee.

Glioma–initiating cell mouse model

Unsorted tumor cells were obtained from human glioblastomas in stage IV. Cells were cultured as floating colonies (gliomaspheres) in Dulbecco's modified Eagle's Medium/F12 containing B27 (1/50), epidermal growth factor and basic fibroblast growth factor (10 ng/mL). Prior to implantation into NOD-scid immunodeficient mice, the number of viable cells was determined by counting cells using trypan blue exclusion. Seven NOD-scid mice injected in the striatum with human GIC (number of passages > 11, number of cells 7×10^4), referred to as CGIC, were scanned every 2 weeks after the injection until tumor formation.

In vivo ^{1}H MRS protocol

All experiments were carried out on an animal 26-cm-diameter, horizontal-bore 14.1-T magnet (Magnex Scientific, Oxford, UK) interfaced to a Direct Drive console (Varian Inc., Palo Alto, CA, USA). The magnet was equipped with a 12-cm-inner-diameter gradient (400 mT/m in 120 µs; Magnex Scientific). A custom-made quadrature surface coil, consisting of two geometrically decoupled 14-mm diameter single loops, was used as a transceiver.

The mice were anesthetized with 3% isoflurane combined with a mixture of air and O_2, stereotaxically fixed with two ear pieces and a bite bar in a holder and placed at the isocenter of the magnet. Throughout the experiment, the mice were kept anesthetized with 1.5–2% isoflurane. Breathing and temperature parameters were monitored with an MR-compatible monitor system (model 1025; SA Instruments, Stony Brook, NY, USA), and animal temperature was maintained at 36.5–37.5°C by circulating warm water.

For localization of the volume of interest (VOI), multi-slice T_2-weighted imaging was performed using the fast spin echo technique with a field of view of 25×25 mm^2, data matrix 256^2, slice thickness 0.8 mm, an effective echo time (TE) of 52 ms, and a repetition time (TR) of 5000 ms.

Before the spectroscopy measurements, the static magnetic field homogeneity was adjusted using first- and second-order shims with an EPI version of FASTMAP (Gruetter and Tkác 2000).

In vivo macromolecule spectrum acquisition and post–processing in the healthy mouse brain

The brain MM spectrum was acquired using SPECIAL (Mlynarik *et al.* 2006) with a 2 ms full-passage hyperbolic secant adiabatic RF inversion pulse applied before the localization sequence (Mlynarik *et al.* 2008). The sequence was combined with a VAPOR water suppression scheme interleaved with outer volume saturation modules (Tkac *et al.* 1999). Differences in T_1 relaxation were used to discriminate residual metabolite signals from the MM spectrum in series of IR acquisitions with TI varying from 600 to 900 ms using shorter and longer echo time (TE = 2.8 and 40 ms) and a TR of 2.5 s. Series of IR acquisitions were also used to determine the best TI to minimize the metabolite signals. An averaging of 1024 repetitions was acquired for each spectrum in a series of IR scans. The MM signals were then acquired with a TI of 775 ms, a TE of 2.8 ms, a TR of 2.5 s and an averaging of 2048 repetitions.

The spectrum of pure MM was obtained after removal of the residual metabolite signals in the metabolite-nulled spectra obtained at TI = 775 ms. Residual metabolite peaks were removed using AMARES (advanced method for accurate, robust, and efficient spectral fitting) (Vanhamme *et al.* 1997), where constraints on peak frequency, phase, linewidth, and amplitude were set to fit the residual peaks to be removed. The setting of the constraints was based on prior knowledge of the frequency, phase and *in vivo* linewidth of the residual metabolite peaks while allowing a small degree of freedom to take experimental condition and physiological effects into account. The MM spectrum devoid of any residual metabolite signal corresponds to the 'residue' in AMARES (which is obtained in AMARES after subtraction of the fitted residual peaks, the 'estimate' in AMARES, from the metabolite-nulled spectrum). Manual iterative fitting was then performed to improve the accuracy of the estimate of the residual metabolite peaks at each step by redefining stronger constraints on the amplitude and linewidth of the residual peaks to fit. The previous residual peak estimate and corresponding MM spectrum, if still considered not completely devoid of metabolite contributions, were used to visually determine which parameter should be refined or modified for better peak fitting of the residual metabolite contribution. An accurate MM spectrum was considered to be obtained when the metabolite contribution to the MM spectrum was visually minimized. Since this procedure had to be manually repeated for each measured MM spectrum to post-process, a set of prior knowledge (on the number of peaks, peak frequency, phase and relative linewidth between peaks) associated with constraints, soft enough to be reused for each new procedure (providing similar experimental conditions), was carefully established to reduce the time needed for the procedure. The use of such prior knowledge may furthermore provide a way to limit any potential operator influence on the post-processing step. For comparison with this newly proposed post-processing method, the residual metabolite peaks were also removed with HLSVD (Pijnappel *et al.* 1992).

Assessment of post-processing and regional effects on the macromolecule contribution

Brain MM spectra were obtained (using the post-processing described above) in several regions of three healthy mice after acquisition of metabolite-nulled spectra in the striatum (STR, VOI = 8 μL), hippocampus (HIP, VOI = 6.75 μL) and in a region, referred to here as mixed-tissue region, that included tissues of several brain structures (MIX, VOI = 27 μL), partially including striatum and hippocampus, using the same acquisition parameters as describe above. Localized ^{1}H MR spectra were acquired using the SPECIAL sequence (TE = 2.8 ms; TR = 4000 ms, 512 repetition scans) in the striatum and hippocampus of those mice.

In vivo ^{1}H spectra were processed as previously described (Mlynarik et al. 2008), frequency drift corrected, summed, and eddy-current compensated using the water signal from the same VOI. The experimental spectra were fitted with LCModel (Provencher 1993), using a simulated basis set of metabolites and MM signals measured in vivo using an inversion-recovery sequence and post-processed as described above. The metabolite basis set included alanine (Ala), ascorbate (Asc), aspartate (Asp), creatine (Cr), myo-inositol (myo-Ins), gamma-aminobutyric acid (GABA), glucose (Glc), glutamine (Gln), glutamate (Glu), glycine (Gly), glycerophosphocholine (GPC), glutathione (GSH), lactate (Lac), N-acetyl-aspartate (NAA), N-acetyl-aspartyl-glutamate (NAAG), phosphocholine (PCho), phosphocreatine (PCr), phosphorylethanolamine (PE), scyllo-inositol (Scyllo), and taurine (Tau).

Absolute quantification of the ^{1}H spectra was performed using the water signal as an internal reference. The water spectra were acquired with the same parameters, without water suppression and with eight averaging scans.

In vivo macromolecule spectrum acquisition and metabolite quantification in the glioma-initiating cell mouse model

Brain MM spectra were measured inside the tumor of seven mice between 8 and 9 weeks post-injection of the CGIC. At this growth stage, the tumor had a size that allowed the location of a VOI of 10–16 μL entirely within the tumor. Metabolite-nulled spectra were acquired in the tumor VOI, which was located in a mixed-tissue region that mostly included striatum and hippocampus tissues (TI = 775 ms, TE = 2.8 ms, TR = 2.5 s, 2048 averages). ^{1}H metabolite spectra were also acquired in an 8 μL volume inside the tumor (TE = 2.8 ms; TR = 4000 ms, 512 averages).

To detect potential alterations of the MM signals in the brain tumor tissue compared to healthy brain tissue, metabolite spectra acquired in the tumors were quantified using both the MM spectrum of the tumor tissue, which was considered to be the closest to the true MM spectrum, and a MM spectrum obtained in the same brain region (mixed tissues) of a healthy mouse.

Statistical analyses

To detect differences in the MM spectra that significantly affect metabolite quantification because of the used MM post-processing methods, metabolite striatum spectra acquired in the healthy mice were quantified using MM spectra obtained after AMARES and HLSVD post-processing. The two types of quantification were performed on each mouse metabolite spectrum of the entire group before a paired Student's t-test was applied on the two types of quantification to detect significant differences in the quantification results.

To detect differences in MM signals between different brain regions that might significantly affect metabolite quantification, the same metabolite spectrum acquired in the striatum (or hippocampus) was quantified with a MM spectrum obtained in the specific region and in a bigger VOI that included several brain tissues (mixed-tissue region). The two types of quantification were performed on each mouse spectrum in the entire group before a paired Student's t-test was applied on the two types of quantification to detect significant differences.

In addition, to determine whether differences between MM spectra of mice and rats significantly affect metabolite quantification, a paired Student's t-test was applied to the metabolite quantification results of each mouse in the entire healthy mouse group obtained after using a mouse and a rat MM spectrum from a mixed-tissue region.

Finally, to detect whether significant alterations of the MM signals in the tumor tissue affected metabolite quantification, the two types of quantification, using the MM spectrum of the tumor tissue and the MM spectrum obtained in a healthy mouse, were performed over the entire group, and a paired Student's t-test was applied to determine the significance of their differences.

Results

Optimization of the macromolecule spectrum acquisition and post-processing in the healthy mouse brain

The optimal TI for measuring metabolite-nulled spectra was determined to be 775 ms, as a result of the overall minimization of the residual metabolite signals, although the different T_1 relaxation times of the metabolite resonances prevented a complete nulling of all the metabolite signals. The negative residual metabolite peaks in the IR series, as well as the residual signals detected at long echo-time IR acquisition, were used to identify the residual peaks that needed to be removed from the metabolite-nulled spectra.

Residual metabolite removal with AMARES versus HLSVD

The new MM post-processing method proposed in this study consisted of using AMARES to fit the residual metabolite peaks in the metabolite-nulled spectra before removing their contribution from the measured spectrum to finally obtain an accurate MM spectrum (Fig. 1a). The possibility of including prior knowledge for the fitting of residual metabolite peaks associated with the manual iteration of the method for refining constraints on the frequency, amplitude, and linewidth of the estimated metabolite residuals until an optimized assessment of their estimation was obtained, allowed for the reliable estimation and removal of all residual metabolite peaks in all cases (Fig. 1b and c).

For comparison, a metabolite-nulled spectrum acquired in the mixed-tissue region and processed with HLSVD is shown in Fig. 2a. The lack of constraints on the amplitude and linewidth of the estimated peaks in HLSVD led to clear differences in the removal of several residual metabolite peaks when compared with the AMARES method, as
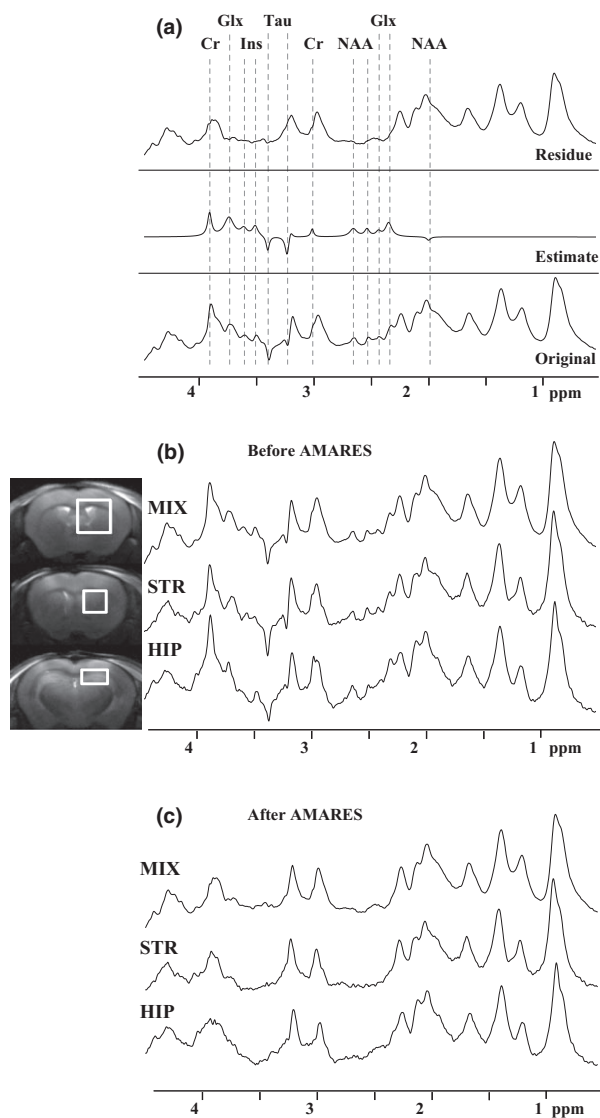
Fig. 1 (a) Application of AMARES (advanced method for accurate, robust, and efficient spectral fitting) for the proposed macromolecule (MM) post-processing method. Residual metabolite peaks (dotted lines) are selected in the acquired metabolite-nulled (original) spectrum and fitted using the available constraints on their frequency, phase, linewidth, and amplitude. Once the optimal estimate of the residual metabolite peaks is reached after several fitting iterations with constraint optimization, the AMARES residue corresponds to the MM spectrum. (b) Metabolite-nulled spectra were acquired in the hippocampus (HIP), striatum (STR) and in a mixed-tissue region (MIX) of a healthy mouse. The residual metabolites can be clearly observed. The location of the volume of interest (VOI) is shown on the anatomical images on the left. (c) The corresponding post-processed MM signals no longer contain the residual metabolites.

visually apparent at e.g., 3.91 ppm (Cr), 3.25 ppm (Tau) and 2.34 ppm (Glu).

Quantification of the striatum metabolite spectra using the MM signals processed using AMARES and HLSVD allowed the reliable measurement of 15 metabolite concentrations with Cramer-Rào lower bounds (CRLB) smaller than 10% (Fig. 2b). However, although MM signals processed with AMARES allowed a reliable quantification of PCho and GPC, this was not the case when using MM signals processed with HLSVD. Only results for tCho are, therefore, reported. In addition, Scyllo, NAAG, and Asp were quantified, but their quantification reliability was lower in general (both when AMARES and HLSVD was used) and some data had to be excluded (CRLB > 30%), leading to a too small sample size that was not included in the statistical analysis. The statistical analysis performed on the quantifications obtained with the two differently processed MM spectra highlighted several significant quantification differences in GABA, Glu, Gly, Ins, Tau and tCho. Those metabolite concentrations were found to be 20%, 7%, 29%, 13%, 13% ($p < 0.05$) and 35% ($p < 0.01$) lower, respectively, when using HLSVD for MM spectra post-processing.

The effect of regional macromolecule differences on metabolite quantification

The MM spectra obtained from metabolite-nulled spectra acquired in the hippocampus, striatum, and in a mixed-tissue region showed no major visually detectable differences (Fig. 3a and b). The statistical analysis of the measured metabolite concentrations likewise showed no statistically significant differences when different MM spectra were used for the metabolite quantification of a given VOI (Fig. 3c and d). The concentration differences were below 10% for most of the metabolites in both striatum and hippocampus areas. Note that in the hippocampus larger, although non-significant, differences were found for Asc, Gly and PE (15–40%). The signal of these metabolites partially overlaps with the MM group that resonates at 3.9 ppm and which has a slightly different shape in the mixed-tissue region and in the hippocampus.

The additional quantification of metabolite spectra acquired in both hippocampus and striatum regions performed using a general rat brain MM spectrum resulted in similar metabolite concentrations compared to when using the regional mouse brain MM spectra. In addition, the statistical analysis between both metabolite quantifications did not reveal any significant difference in the metabolite concentration measured when either the regional MM spectrum or the general rat brain MM spectrum was used (Fig. 3c and d).

In vivo MM spectrum acquisition in a glioma–initiating cell mouse model and metabolite quantification

Based on a series of IR spectra, TI of 775 ms was determined to be optimal for nulling metabolites within the brain tumor, similar to the healthy mouse TI. Residual metabolite signals were efficiently removed with AMARES as described above for the healthy mouse. The MM spectra obtained from the GIC mice showed visually clearly discernible differences

Fig. 2 (a) From bottom to top: a metabolite-nulled spectrum acquired with TI = 775 ms in the mixed-tissue region of a healthy mouse and the same macromolecule (MM) spectrum post-processed using either Hankel-Lanczos singular value decomposition (HLSVD) or AMARES (advanced method for accurate, robust, and efficient spectral fitting), respectively. Dotted lines indicate the more prominent differences in residual peaks removal for creatine (Cr), taurine (Tau) and glutamate (Glu). Note for example the removal of the macromolecule peak next to creatine. (b) Metabolite quantification of the striatum (STR) metabolite spectra (*n* = 3) using the MM spectra obtained either after AMARES or HLSVD post-processing. Significant metabolite quantification differences between both methods are indicated with *p < 0.05 and **p < 0.01. Error bars represent the SD.
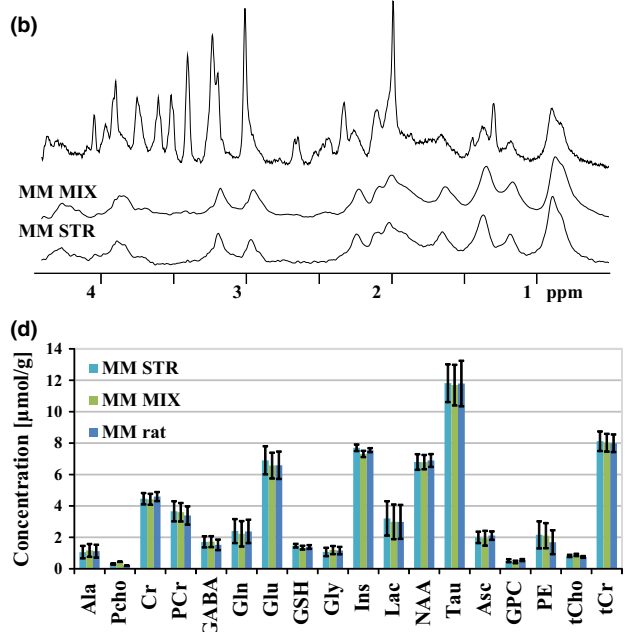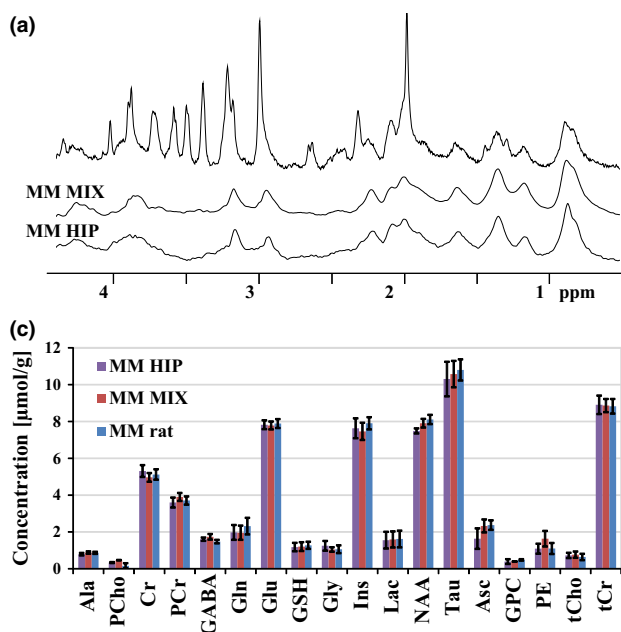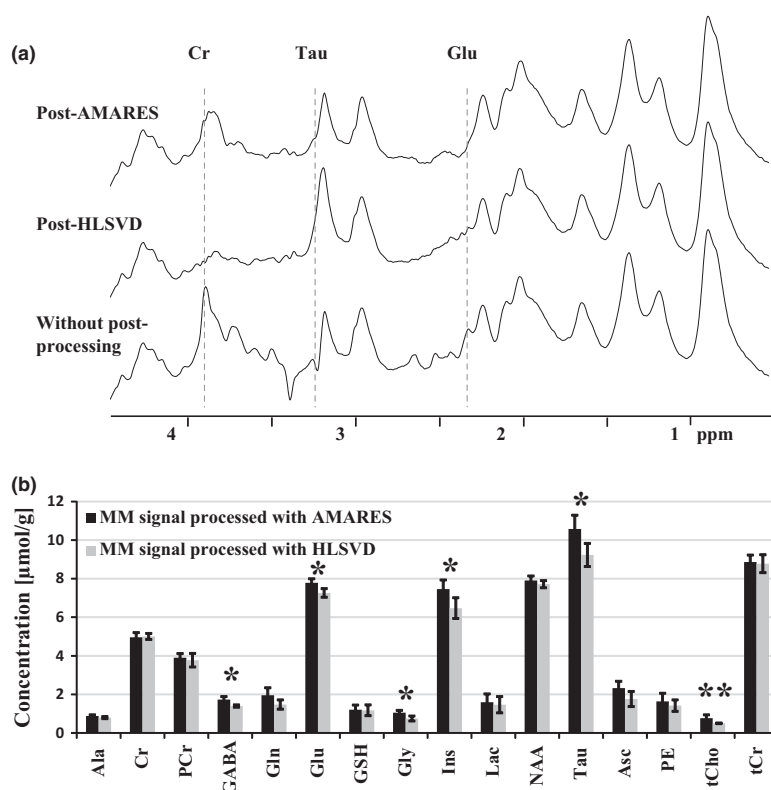

Fig. 3 Spectra acquired in the hippocampus (HIP) (a) and in the striatum (STR) (b) of a healthy mouse with the macromolecule (MM) signals acquired in the same brain region (HIP or STR) or in a mixed-tissue region (MIX). (c and d) Metabolite quantification results (*n* = 3) using either the MM signal from the same brain region, the mixed-tissue region or from a rat mixed-tissue brain region. Metabolite levels are displayed with error bars representing the SD of the measurement. No visually apparent significant differences can be observed in the MM spectra, and similarly no statistically significant differences were observed in the quantified concentrations.

from the MM obtained in healthy mice (Fig. 4). Additional peaks, not present in healthy mouse MM spectra, were detected at 1.3 and 2.8 ppm in the MM spectra of GIC mice. Moreover, the GIC mouse spectra demonstrated an increase in the MM component between 3.5 and 3.7 ppm compared to healthy mouse MM spectra. An increased variability in the MM spectrum was also observed in the GIC mice, which was ascribed to brain MM modifications associated with the glioma, of which the development stage was slightly different in each mouse.

The quantifications of the tumor spectra performed using the MM spectrum from a healthy brain mixed-tissue region and from the investigated mouse tumor to detect whether significant quantification bias was caused by neglecting to take brain MM signals alterations that occur in tumorous tissues into account showed several qualitative differences. While all the metabolites included in the basis set except Glc and GPC were reliably quantified (CRLB < 30%) when the tumor MM spectrum was used, three metabolites, Ala, GSH, and NAAG, failed to be quantified when the healthy tissue MM spectrum was used. Moreover, all metabolites were
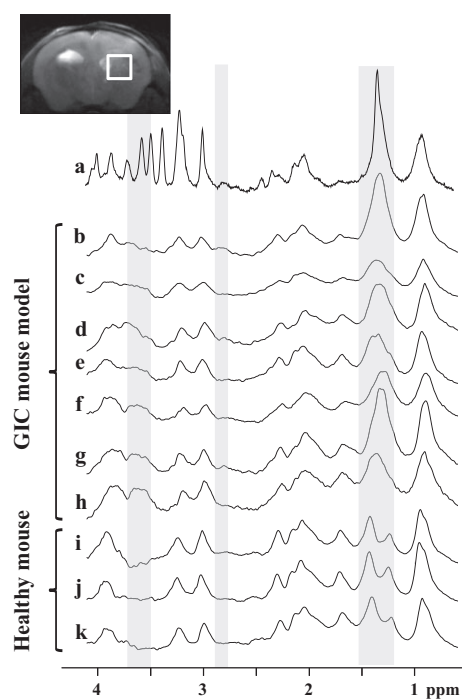
quantified with higher CRLB when the MM spectrum acquired from healthy tissue was used. Furthermore, this quantification resulted in non-noise residuals and a distorted baseline, including a consistently positive baseline distortion between 3.6 and 3.7 ppm. This distortion corresponded to the spectral region where an increase in MM signals of the tumor tissue was observed. These residuals and distortion were minimized when the MM spectrum from the tumor was used. The statistical analysis performed on both quantifications resulted in the detection of significant differences in the measured metabolite concentrations (Table 1). Asp was significantly underestimated with 23%, while Lac was significantly overestimated with 61% when the healthy tissue MM spectrum was used ($p < 0.003$). Moreover, several statistically non-significant trends were detected such as an overestimation of 11% of PCr ($p < 0.09$), 31% of PCho ($p < 0.06$) and 29% of Glu ($p < 0.09$), as well as an underestimation of 18% of the GABA level ($p < 0.06$).

Discussion

In this study, we presented a novel method for the post-processing of the measured MM spectra to achieve an

Fig. 4 (a) Metabolite spectrum acquired in the tumor region of a glioma-initiating cell (GIC) mouse displayed with the volume of interest (VOI) in the tumor indicated on a T_2-weighted image (inset). Macromolecule (MM) signals of brain tumors in seven GIC mice are displayed underneath (b–h). For comparison, three brain MM signals acquired in the same brain region of healthy mice are also displayed (i–k). The shaded areas indicate visual differences in the shape of the MM signals between healthy and GIC mice at 3.6–3.7 ppm and 1.3 ppm. Differences were also observed at 2.8 ppm but only in some of the GIC mice.

Table 1 Metabolite quantification differences in the GIC mice ($n = 7$) when a healthy mouse MM spectrum was used instead of the specific MM spectrum acquired within the mouse tumor

Metabolite	Quantification difference [%]	Concentration [μmol/g]
Asp	−23 ± 5*	1.10 ± 0.40
PCho	+31 ± 35	0.88 ± 0.24
Cr	−9 ± 20	2.94 ± 1.13
PCr	+11 ± 14	2.45 ± 0.25
GABA	−18 ± 8	0.66 ± 0.17
Gln	−7 ± 17	2.51 ± 1.02
Glu	+29 ± 39	4.11 ± 0.77
Gly	+39 ± 64	2.53 ± 1.83
Ins	+5 ± 16	9.24 ± 2.98
Lac	+61 ± 31*	13.23 ± 4.32
NAA	+20 ± 40	1.72 ± 0.39
Scyllo	−5 ± 30	0.34 ± 0.10
Tau	−2 ± 7	11.35 ± 2.89
Asc	0 ± 46	2.55 ± 1.33
PE	+13 ± 27	2.53 ± 0.69
tNAA	−5 ± 23	1.93 ± 0.31
Glu+Gln	+12 ± 19	6.62 ± 1.51
tCho	+4 ± 25	0.90 ± 0.28
tCr	+6 ± 8	5.50 ± 0.93

The average metabolite concentration difference obtained in seven GIC mice is displayed with the SD of this difference. The significance of the difference of the metabolite quantification is indicated by *$p < 0.003$. In addition, metabolite concentrations measured in the tumor of the GIC mouse model ($n = 7$) when the specific tumor MM spectra were used for quantification are also displayed.

improved assessment of the MM spectrum through an accurate separation and removal of the residual metabolite peaks from the MM component. Potential regional and pathological differences that might affect the MM spectrum of the mouse brain and, therefore, the quantification accuracy were investigated.

The novel method proposed for the post-processing of MM spectra based on AMARES was used for a robust removal of the residual metabolite peaks from the MM component. The high flexibility of the AMARES method, which allows the definition of constraints on the linewidth, frequency, phase, and amplitude of the components used for the fitting of the metabolite residuals, appears to be more successful than HLSVD in discriminating residual metabolite signals from the MM components. Indeed, as can for example be seen in Fig. 2a for the 3.9 ppm creatine peak, HLSVD did not consistently succeed in separating metabolite from MM resonances when the metabolite had a positive phase and the MM component underneath had a relative narrow linewidth. On the contrary, the possibility of putting constraints on the linewidth and amplitude of the residual metabolite peaks in AMARES consistently allowed the robust separation of the residuals from the MM resonances, even in the case of relative narrow MM resonance linewidth. In other cases when small metabolite contributions were difficult to estimate, the IR series helped to establish the reliability of the MM signal. However the IR series is not always available because of time limitations and, in its absence, metabolite residual contributions such as those of Glu and Tau might be difficult to estimate as a result of their location on the MM resonance peaks. When HLSVD was used, it was indeed difficult to evaluate the correct MM signal shape and if the metabolite residuals were correctly estimated. The advantage of AMARES over HLSVD is that by varying the fit constraints, residual metabolite peaks could be virtually over- or underestimated such that the best fits of the residual metabolite peaks were obtained when the residual signal was exactly compensated. An imperfect removal of these metabolite residuals with HLSVD was furthermore suggested by the significant differences detected in the quantification results when AMARES was used instead of HLSVD for the MM post-processing.

The statistical analysis of the metabolite quantification using AMARES and HLSVD post-processed MM spectra showed not only significant quantification differences in metabolites that overlap with the MM components but also for other metabolites such as Gly, which suggests that the accuracy of the removal of residual metabolite signals in the MM spectrum significantly affects the quantification of many metabolites, especially those that have a weaker representation in the spectra. As such, the AMARES method, which offers a greater flexibility for the accurate fitting of residual metabolite peaks, appears to be the best alternative for the post-processing of the MM components. An accurate

measurement of the MM spectrum is especially crucial for a reliable metabolite level monitoring in specific cases when the MM spectrum is altered and changes with disease progression such as in stroke, multiple sclerosis, and tumors (Graham *et al.* 2001; Mader *et al.* 2001; Howe *et al.* 2003; Opstad *et al.* 2010).

The investigation of potential regional differences that might affect the healthy mouse brain MM signals, similar to what has been observed in the rat brain (Xin *et al.* 2010a), showed that no difference between the MM signals of different brain regions has a significant impact on the quantification of the brain metabolites. Indeed, the MM spectra were shown to be very similar throughout the different brain regions and the few slight variations of the MM signals observed between different brain regions were shown to not significantly affect metabolite quantification. Most of the metabolites were quantified with differences lower than 10% when using the mixed-tissue instead of the region-specific MM spectrum, which is within the typical SD of the concentration measurement. Higher differences were obtained only for a few low-concentration metabolites (Asc, Gly, PE) that were quantified with lower precision, which explains these higher differences in quantification. These results thus suggest that a unique MM spectrum acquired in a fairly large region that contains mixed tissues of a healthy mouse brain can be generally used for the brain metabolite quantification of any brain region in a healthy mouse. The similar results obtained when comparing the quantification using either the mouse or the rat MM spectrum of similar brain areas suggest that this can be generalized to the use of a region-non-specific rat or mouse brain MM spectrum for quantification of metabolites in healthy animal brains of both species.

Since brain pathologies may alter the MM and brain lipid content (Graham *et al.* 2001; Mader *et al.* 2001; Howe *et al.* 2003; Seeger *et al.* 2003; Opstad *et al.* 2010), we studied a mouse model of human brain glioma. In several mice of this glioma-initiating-cell model, MM peaks that were not detected in the brain of healthy mice were observed at 1.3 ppm and at 2.8 ppm. These signals correspond to mobile lipid signals that have already been observed in previous *in vivo* and *in vitro* studies on human and animal model brain gliomas (Remy *et al.* 1997; Hakumaki *et al.* 1999; Auer *et al.* 2001; Howe *et al.* 2003; Opstad *et al.* 2010). Those signals, when not taken into accounts in the MM spectrum or other basis sets, led to significant errors in quantification of Lac and Asp, which overlap with the neglected lipid signals. Although the presence of the mobile lipid peak at 1.3 ppm is well known and has generally been taken into account in quantification in previous investigations of brain gliomas using either simulated or parameterized lipid resonances (Auer *et al.* 2001; Seeger *et al.* 2003; Opstad *et al.* 2010; Doblas *et al.* 2012), the presence of lipids at 2.8 ppm has been rarely included in the quantification of *in vivo* spectra

(Seeger *et al.* 2003; Opstad *et al.* 2010). However, our results demonstrated the importance of taking its contribution into account, especially when Asp quantification is of interest.

Moreover, a modification in the MM spectrum was detected in the spectral region at 3.6–3.7 ppm in the tumor brain tissue, with the presence of a broad signal that was not observed in any brain region studied in the healthy mouse. This MM signal modification has not been observed in previous studies, as none of them measured the MM spectrum at such high magnetic field strength. Indeed, unlike the lipid signals, the MM signals in brain gliomas have been measured in only a few studies (Howe *et al.* 2003; Seeger *et al.* 2003) that were performed at low magnetic field strength and longer echo time, where the MM contribution is minimized and poorly resolved. Both these aspects contributed to an increased difficulty to detect small or smooth changes in the MM signals at low magnetic field strength and/or longer echo time, where such slight changes may have a lower impact on metabolite quantification than at higher magnetic field strength. Moreover, the broad MM resonance observed between 3.6 ppm and 3.7 ppm does not correspond to any mobile lipid signal reported in previous studies performed *in vitro* on glioma cells or *in vivo* on brain gliomas (Hakumaki *et al.* 1999; Delikatny *et al.* 2011; Mirbahai *et al.* 2012). This modification might be a result of structural changes of the MM components because of the tumor. Further investigations are needed to be able to explain the presence of this MM signal in glioma tissue, which may be of interest for an improved characterization of gliomas. However, the oversight of this additional MM component in the MM spectrum did not lead to any significant error in the metabolite quantification, since LCModel was able to compensate for this neglected contribution in the spectra in the quantification baseline. The resulting distorted baseline, however, may provide an explanation for the generally lower reliability of the metabolite quantification (higher CRLB and fewer metabolites successfully quantified) that was observed when a non-complete MM spectrum was used.

We conclude that the novel MM post-processing method based on AMARES presented in this study provides an efficient way to accurately separate and remove the residual metabolite peaks from the measured MM component and therefore provides an improved *in vivo* assessment of the pure MM spectrum. We further conclude from the obtained results using this optimized method that a unique non-specific brain MM spectrum can be used for a general quantification of healthy mouse or rat brain metabolite spectra. Finally, we conclude that an accurate assessment of the modifications in the MM contribution in glioma spectra that were seen not limited to lipid signals, is necessary for reliable metabolite quantification, while it might also provide an additional characterization of the pathology.

References

Auer D. P., Gossl C., Schirmer T. and Czisch M. (2001) Improved analysis of 1H-MR spectra in the presence of mobile lipids. *Magn. Reson. Med.* **46**, 615–618.

Behar K. L. and Ogino T. (1993) Characterization of Macromolecule Resonances in the H-1-Nmr Spectrum of Rat-Brain. *Magn. Reson. Med.* **30**, 38–44.

Cudalbu C., Bucur A., Graveron-Demilly D., Beuf O. and Cavassila S. (2007) Comparison of two strategies of background-accommodation: influence on the metabolite concentration estimation from in vivo Magnetic Resonance Spectroscopy data. *Conf. Proc. IEEE Eng. Med. Biol. Soc.* **2007**, 2077–2080.

Cudalbu C., Mlynarik V., Xin L. and Gruetter R. (2009a) Comparison of T1 relaxation times of the neurochemical profile in rat brain at 9.4 tesla and 14.1 tesla. *Magn. Reson. Med.* **62**, 862–867.

Cudalbu C., Mlynarik V., Xin L. and Gruetter R. (2009b) Quantification of in vivo short echo-time proton magnetic resonance spectra at 14.1 T using two different approaches of modelling the macromolecule spectrum. *Meas. Sci. Technol.* **20**, 104034.

Delikatny E. J., Chawla S., Leung D. J. and Poptani H. (2011) MR-visible lipids and the tumor microenvironment. *NMR Biomed.* **24**, 592–611.

Doblas S., He T., Saunders D., Hoyle J., Smith N., Pye Q., Lerner M., Jensen R. L. and Towner R. A. (2012) In vivo characterization of several rodent glioma models by 1H MRS. *NMR Biomed.* **25**, 685–694.

Fan G., Sun B., Wu Z., Guo Q. and Guo Y. (2004) In vivo single-voxel proton MR spectroscopy in the differentiation of high-grade gliomas and solitary metastases. *Clin. Radiol.* **59**, 77–85.

Gottschalk M., Lamalle L. and Segebarth C. (2008) Short-TE localised 1H MRS of the human brain at 3 T: quantification of the metabolite signals using two approaches to account for macromolecular signal contributions. *NMR Biomed.* **21**, 507–517.

de Graaf R. A., Brown P. B., McIntyre S., Nixon T. W., Behar K. L. and Rothman D. L. (2006) High magnetic field water and metabolite proton T1 and T2 relaxation in rat brain in vivo. *Magn. Reson. Med.* **56**, 386–394.

Graham G. D., Hwang J. H., Rothman D. L. and Prichard J. W. (2001) Spectroscopic assessment of alterations in macromolecule and small-molecule metabolites in human brain after stroke. *Stroke* **32**, 2797–2802.

Gruetter R. and Tkác I. (2000) Field mapping without reference scan using asymmetric echo-planar techniques. *Magn. Reson. Med.* **43**, 319–323.

Hakumaki J. M., Poptani H., Sandmair A. M., Yla-Herttuala S. and Kauppinen R. A. (1999) 1H MRS detects polyunsaturated fatty acid accumulation during gene therapy of glioma: implications for the in vivo detection of apoptosis. *Nat. Med.* **5**, 1323–1327.

Hong S. T. and Pohmann R. (2013) Quantification issues of in vivo (1) H NMR spectroscopy of the rat brain investigated at 16.4 T. *NMR Biomed.* **26**, 74–82.

Hong S. T., Balla D. Z., Shajan G., Choi C., Ugurbil K. and Pohmann R. (2011) Enhanced neurochemical profile of the rat brain using in vivo (1)H NMR spectroscopy at 16.4 T. *Magn. Reson. Med.* **65**, 28–34.

Howe F. A., Barton S. J., Cudlip S. A. *et al.* (2003) Metabolic profiles of human brain tumors using quantitative in vivo 1H magnetic resonance spectroscopy. *Magn. Reson. Med.* **49**, 223–232.

Kauppinen R. A., Kokko H. and Williams S. R. (1992) Detection of mobile proteins by proton nuclear-magnetic-resonance spectroscopy in the guinea-pig brain exvivo and their partial-purification. *J. Neurochem.* **58**, 967–974.

Kauppinen R. A., Niskanen T., Hakumaki J. and Williams S. R. (1993) Quantitative-analysis of h-1-NMR detected proteins in the rat cerebral-cortex in-vivo and in-vitro. *NMR Biomed.* **6**, 242–247.

Kuesel A. C., Sutherland G. R., Halliday W. and Smith I. C. (1994) 1H MRS of high-grade astrocytomas: mobile lipid accumulation in necrotic tissue. *NMR Biomed.* **7**, 149–155.

Kunz N., Cudalbu C., Mlynarik V., Huppi P. S., Sizonenko S. V. and Gruetter R. (2010) Diffusion-weighted spectroscopy: a novel approach to determine macromolecule resonances in short-echo time 1H-MRS. *Magn. Reson. Med.* **64**, 939–946.

Lei H. X., Poitry-Yamate C., Preitner F., Thorens B. and Gruetter R. (2010) Neurochemical profile of the mouse hypothalamus using in vivo H-1 MRS at 14.1T. *NMR Biomed.* **23**, 578–583.

Mader I., Seeger U., Weissert R., Klose U., Naegele T., Melms A. and Grodd W. (2001) Proton MR spectroscopy with metabolite-nulling reveals elevated macromolecules in acute multiple sclerosis. *Brain* **124**, 953–961.

Mader I., Seeger U., Karitzky J., Erb M., Schick F. and Klose U. (2002) Proton magnetic resonance spectroscopy with metabolite nulling reveals regional differences of macromolecules in normal human brain. *J. Magn. Reson. Imaging* **16**, 538–546.

Mirbahai L., Wilson M., Shaw C. S., McConville C., Malcomson R. D., Kauppinen R. A. and Peet A. C. (2012) Lipid biomarkers of glioma cell growth arrest and cell death detected by 1 H magic angle spinning MRS. *NMR Biomed.* **25**, 1253–1262.

Mlynarik V., Gambarota G., Frenkel H. and Gruetter R. (2006) Localized short-echo-time proton MR spectroscopy with full signal-intensity acquisition. *Magn. Reson. Med.* **56**, 965–970.

Mlynarik V., Cudalbu C., Xin L. and Gruetter R. (2008) 1H NMR spectroscopy of rat brain in vivo at 14.1Tesla: improvements in quantification of the neurochemical profile. *J. Magn. Reson.* **194**, 163–168.

Murphy P. S., Rowland I. J., Viviers L., Brada M., Leach M. O. and Dzik-Jurasz A. S. (2003) Could assessment of glioma methylene lipid resonance by in vivo (1)H-MRS be of clinical value? *Br. J. Radiol.* **76**, 459–463.

Opstad K. S., Wright A. J., Bell B. A., Griffiths J. R. and Howe F. A. (2010) Correlations between in vivo (1)H MRS and ex vivo (1)H HRMAS metabolite measurements in adult human gliomas. *J. Magn. Reson. Imaging* **31**, 289–297.

Otazo R., Mueller B., Ugurbil K., Wald L. and Posse S. (2006) Signal-to-noise ratio and spectral linewidth improvements between 1.5 and 7 Tesla in proton echo-planar spectroscopic imaging. *Magn. Reson. Med.* **56**, 1200–1210.

Pfeuffer J., Tkac I., Provencher S. W. and Gruetter R. (1999) Toward an in vivo neurochemical profile: quantification of 18 metabolites in short-echo-time (1)H NMR spectra of the rat brain. *J. Magn. Reson.* **141**, 104–120.

Pijnappel W. W. F., Vandenboogaart A., Debeer R. and Vanormondt D. (1992) Svd-based quantification of magnetic-resonance signals. *J. Magn. Reson.* **97**, 122–134.

Provencher S. W. (1993) Estimation of metabolite concentrations from localized in vivo proton NMR spectra. *Magn. Reson. Med.* **30**, 672–679.

Remy C., Fouilhe N., Barba I. *et al.* (1997) Evidence that mobile lipids detected in rat brain glioma by 1H nuclear magnetic resonance correspond to lipid droplets. *Cancer Res.* **57**, 407–414.

Schaller B., Xin L. and Gruetter R. (2012) Influence of tissue specific macromolecule baseline on the metabolite quantification in human brain at 7 Tesla. *Proc. Int. Soc. Magn. Reson. Med.* **20**, 1774.

Schaller B., Xin L. J., Cudalbu C. and Gruetter R. (2013) Quantification of the neurochemical profile using simulated macromolecule resonances at 3 T. *NMR Biomed.* **26**, 593–599.

Seeger U., Klose U., Mader I., Grodd W. and Nagele T. (2003) Parameterized evaluation of macromolecules and lipids in proton MR spectroscopy of brain diseases. *Magn. Reson. Med.* **49**, 19–28.

Soher B. J., Young K. and Maudsley A. A. (2001) Representation of strong baseline contributions in 1H MR spectra. *Magn. Reson. Med.* **45**, 966–972.

Tkac I., Starcuk Z., Choi I. Y. and Gruetter R. (1999) In vivo H-1 NMR spectroscopy of rat brain at 1 ms echo time. *Magn. Reson. Med.* **41**, 649–656.

Tkac I., Rao R., Georgieff M. K. and Gruetter R. (2003) Developmental and regional changes in the neurochemical profile of the rat brain determined by in vivo H-1 NMR spectroscopy. *Magn. Reson. Med.* **50**, 24–32.

Vanhamme L., van den Boogaart A. and Van Huffel S. (1997) Improved method for accurate and efficient quantification of MRS data with use of prior knowledge. *J. Magn. Reson.* **129**, 35–43.

Xin L., Mlynarik V., Lei H. X. and Gruetter R. (2010a) Influence of regional macromolecule baseline on rat brain neurochemical profile. *Proc. Int. Soc. Magn. Reson. Med.* **18**, 321.

Xin L. J., Gambarota G., Duarte J. M. N., Mlynarik V. and Gruetter R. (2010b) Direct in vivo measurement of glycine and the neurochemical profile in the rat medulla oblongata. *NMR Biomed.* **23**, 1097–1102.